

# The Neutral Hydrogen Column Density towards Q1937–1009 from the Unabsorbed Intrinsic Continuum in the Lyman- $\alpha$ Forest

SCOTT BURLES<sup>1</sup> & DAVID TYTLER<sup>1</sup>

Department of Physics, and Center for Astrophysics and Space Sciences  
University of California, San Diego  
C0424, La Jolla, CA 92093-0424

## ABSTRACT

The absorption system at  $z = 3.572$  towards Q1937–1009 provides the best extragalactic measurement of the atomic deuterium to hydrogen ratio, D/H. We have obtained a new low-resolution, high signal-to-noise ratio (SNR) Keck spectrum to re-measure the total neutral hydrogen column density  $N(\text{H I})$  using the amount of Lyman continuum absorption. We develop a new method to directly determine the intrinsic unabsorbed quasar continuum from low-resolution spectra of the Ly $\alpha$  forest for the first time. We use three types of spectra to measure  $N(\text{H I})$ : (1) A wide slit spectrum for flux calibration, (2) a high-resolution spectrum to determine the unabsorbed continuum between Ly $\alpha$  forest lines, and (3) a high SNR spectrum to measure the residual flux below the Lyman limit. We measure  $\text{Log } [N(\text{H I})] = 17.86 \pm 0.02 \text{ cm}^{-2}$ , which is reliable because  $N(\text{H I})$  is fully specified by the data. This result is consistent with the  $N(\text{H I})$  measured by Tytler, Fan & Burles (1996) from the Lyman series absorption lines, but not with absorption models proposed by Wampler (1996) nor estimates of the total  $N(\text{H I})$  by Songaila et al. (1997), both of which suggested lower  $N(\text{H I})$  and higher D/H. The Wampler models predict abundant flux below the Lyman limit which is absent from both our old and new spectra, taken with different instruments. The new Keck data is consistent with the data presented by Songaila et al. (1997). The results differ due to the different methods of analysis, and our measurement of the QSO continuum does not agree with the continuum models assumed by Songaila et al. (1997).

---

<sup>1</sup>Visiting Astronomer, W. M. Keck Telescope, California Association for Research in Astronomy

## 1. INTRODUCTION

High-redshift QSO absorption systems can yield measurements of the deuterium-to-hydrogen ratio (D/H) in nearly primordial gas (Adams 1976; Tytler et al. 1996; Burles & Tytler 1996). Recently, limits on D/H have been presented in the range of  $2.3 \times 10^{-5} < \text{D/H} < 24 \times 10^{-5}$  (for a list, see Tytler & Burles 1996). But deuterium is rarely seen in absorption in QSO spectra. Utilizing low resolution spectra of over 300 QSOs to identify systems most likely to show deuterium (Burles et al. 1997), we have found only 2 systems which will provide measures of D/H. No one else has verified a measurement. Because of the small number of systems available, it is efficient to study each in as much detail as possible. In this paper, we continue with our analysis of Q1937–1009.

Tytler, Fan & Burles (1996, hereafter TFB) presented high resolution spectra of Q1937–1009 and a measurement of D/H in the absorption system at  $z = 3.572$ . This system is well suited for a measurement of D/H because the hydrogen has a simple, narrow velocity structure, and the deuterium feature is strong but unsaturated. TFB measured the total neutral hydrogen column density,  $\text{Log} [\text{N(H I)}] = 17.94 \pm 0.06 \pm 0.05 \text{ cm}^{-2}$  (the first error is statistical, and the second is systematic), using a two component Voigt profile fit to the Lyman series absorption lines.

Wampler (1996) has suggested that this hydrogen column density is not well determined, due to either incorrect sky subtraction or improper modeling. He proposed models with 3–6 times less N(H I). Lowering N(H I) does two things: (1) it weakens the absorption in the damping wings of  $\text{Ly}\alpha$ , and (2) it raises the residual flux below the Lyman limit at 4200 Å. N(H I) is difficult to measure from the dampings wings because systematic errors in the assumed unabsorbed QSO continuum level are important. On the other hand, the total N(H I) is well constrained by the residual flux below the Lyman limit.

Songaila et al. (1997) obtained LRIS spectra of Q1937–1009 to determine the total N(H I) at  $z = 3.572$  by measuring the residual Lyman limit flux. The data which they present is consistent with the data which we present below. But the final answers differ because we use different methods. They report a confident upper limit,  $\text{Log} [\text{N(H I)}] < 17.7 \text{ cm}^{-2}$ , which we do not confirm, and our result is not consistent with theirs. We discuss possible reasons for the differences in section 4.

We face two problems with this measurement, and both are due to the absorption of the other unrelated lines in the  $\text{Ly}\alpha$  forest. First, the high number density of the  $\text{Ly}\alpha$  forest lines makes it difficult to determine the intrinsic unabsorbed quasar continuum. Second,  $\text{Ly}\alpha$  absorption clouds at lower redshift contribute to the optical depth below the Lyman limit, which leads to an overestimation of the optical depth at  $z = 3.572$ .

We have obtained data on Q1937–1009 to overcome both these difficulties. We have three spectra, from three different instruments and two different telescopes. We refer to each spectrum by the instrument used: LRIS, HIRES and Kast. Each spectrum provides additional and independent information to measure  $N(\text{H I})$  at  $z = 3.572$ . The LRIS spectrum has high SNR at the wavelengths below the Lyman limit. The HIRES spectrum resolves all the  $\text{Ly}\alpha$  forest lines from  $\text{Ly}\alpha$  emission at  $5830 \text{ \AA}$  to the Lyman limit at  $4200 \text{ \AA}$ , and allows us to measure the local continuum between the unrelated  $\text{Ly}\alpha$  forest absorption lines. The Kast spectrum will provide the absolute flux of Q1937–1009, from the Lyman limit to  $8000 \text{ \AA}$ , which is needed to measure the amount of Lyman continuum absorption.

## 2. OBSERVATIONS & DATA REDUCTION

In this section, we present two new spectra of Q1937–1009: the Kast and LRIS spectra. We discuss the data reduction and the combination of these spectra with the existing HIRES spectrum.

### 2.1. Kast Spectrum for Flux Calibration

Q1937–1009 was observed on the night of August 19, 1996 with the Kast double spectrograph on the Shane 3-m Telescope at Lick Observatory. Two 3000 second exposures were obtained with a  $7''$  wide by  $145''$  long slit and the 600 lines/mm grating on both the red and blue sides. The effective resolution of  $\approx 2''$  is determined by the telescope guiding and seeing. Flat field images were taken immediately after the object exposures to remove the fringing effects redward of  $7000 \text{ \AA}$ . The flux standard BD +33° 2642 was observed in the same setup directly before Q1937–1009. The spectrograph was rotated to align its slit with the average parallactic angle in all observations. The CCD images were overscan corrected, short bias subtracted, and flat-field corrected. The spectrum was optimally extracted from these images in IRAF, and placed on the HIRES wavelength scale (section 2.3). Extinction corrections for the Lick Observatory were applied to both the object and standard star spectra. The spectrum was also dereddened with  $E(\text{B-V}) = 0.18$  and  $R=3.2$  (Burstein & Heiles 1984). Figure 1 shows the final flux calibrated spectrum of Q1937–1009.

## 2.2. LRIS Spectrum

On the night of August 11, 1996, Charles Steidel kindly obtained three 30 minute exposures with the Low Resolution Imaging Spectrograph (LRIS) on the Keck1 10-m Telescope. The observations were made with a 1.0" wide by 180" long slit and a 900 lines/mm grating blazed at 5500 Å. For each observation, the spectrograph was rotated to align its slit with the parallactic angle to reduce slit losses from differential atmospheric refraction. The detector was a Tektronix 2048x2048 pixel CCD with 24  $\mu$ m square pixels. At the Cassegrain focus, each pixel sampled 0.22" square. The CCD images were overscan corrected, short bias subtracted, and flat-field corrected. Each image was background subtracted by fitting a 2nd order Chebyshev polynomial to each column. Fifty pixels along the spatial direction in an 11" region on each side of the object were used in the fits. The three images were then shifted spatially to overlay the object. The three images were coadded and the 1-D spectrum was extracted from this final image. Each pixel in the 1-D spectrum is the sum of pixels in a 6.6" synthetic aperture centered on the object. The aperture center was traced along the object and fit with a 2nd order cubic spline. The  $1\sigma$  error on each pixel includes Poisson errors from the object and background and the readout noise of the CCD. We applied the HIRES wavelength scale described in section 2.3.

An initial flux calibration was accomplished with an extinction corrected spectrum of BD +33° 2642. We then corrected the LRIS flux to match the absolute flux of the Kast spectrum. We smoothed the LRIS spectrum to the Kast spectral resolution, and divided the smoothed LRIS spectrum into the Kast spectrum. A low order polynomial was fit to this response function and applied to the original LRIS spectrum. The response function removes the low-order flux differences between the wide slit and narrow slit spectra. The spectra were overlaid and the overall flux match between the LRIS and Kast spectra were confirmed. The fully reduced LRIS spectrum is shown in Figure 2.

## 2.3. Common Wavelength Scale

Our analysis requires nearly identical wavelength scales on all spectra, hence we transferred the wavelength scale from the existing HIRES spectrum (TFB) to the low resolution LRIS and Kast spectra. We performed the following procedure for the LRIS spectrum. We used a similar procedure to wavelength calibrate the Kast spectrum.

The HIRES spectrum ( $\text{FWHM} = 9 \text{ km s}^{-1}$ ) was smoothed to the LRIS spectral resolution ( $\text{FWHM} = 3.0 \text{ Å}$ ) and rebinned to the LRIS pixel size ( $\Delta\lambda = 0.83 \text{ Å}$ ) and pixel positions. We refer to this spectrum as the Smoothed HIRES spectrum. Unblended

Lyman- $\alpha$  absorption features were identified in the Smoothed HIRES spectrum and were marked in the LRIS spectrum. A 3rd order cubic spline was fit to the positions of the absorption features in the LRIS spectrum, and left an RMS residual of 0.22 pixels. This procedure applied a high resolution wavelength calibration to a low resolution spectrum.

### 3. The Intrinsic Unabsorbed Quasar Continuum

In the LRIS spectrum, the intrinsic unabsorbed quasar continuum level is difficult to determine blueward of Lyman- $\alpha$  emission, because blended Ly $\alpha$  features reduce the observed flux to well below the unabsorbed quasar continuum in nearly all pixels. We avoid this problem by transferring the continuum level from the HIRES spectrum to the LRIS spectrum. The HIRES spectrum resolves the Ly $\alpha$  lines and allows an unbiased estimate of the continuum level in each echelle order (eg. Kirkman & Tytler 1997).

We remove the absorption features in the LRIS spectrum by dividing by the Smoothed HIRES spectrum. Both spectra have very high SNR, and the division produces a fairly well behaved quotient which we show in Figure 3. The result represents the intrinsic unabsorbed continuum of a high redshift QSO, seen for the first time. The break in the continuum near 4650Å (1020 Å rest) agrees with the power-law break seen in composite spectra of low-redshift quasars (Zheng et al. 1997). Lu & Zuo (1994) showed that the unabsorbed continuum in the Ly $\alpha$  forest deviates systematically from the extrapolated continuum. This method does not require a statistical modeling of the absorption spectrum or the extrapolation of the continuum from wavelengths redward of Ly $\alpha$  emission.

#### 3.1. Uncertainty in the Unabsorbed Continuum Level

In Figure 3, the points represent the calculated continuum level in each LRIS pixel. The strong feature at 4920 Å is the QSO Ly $\beta$  -O VI emission feature. The position of Ly $\gamma$  is also marked at 4680 Å. We fit the quasar continuum with least squares minimization and a linear fit,  $I(\lambda) = a(\lambda - 4550\text{Å}) + b$ , between 4250 Å and 4850 Å. The best fit is the solid line in Figure 3, with  $a = 0.0028 \pm 0.0002$  and  $b = 7.76 \pm 0.03$ . The dashed lines represent the  $1\sigma$  errors in the linear coefficients. The linear model gives a good fit to the data, and provides a simple extrapolation to lower wavelengths.

The scatter in the data is approximately twice as large as expected for purely random errors. There are two probable reasons for the increased scatter: (1) intrinsic features in the unabsorbed quasar spectrum, and (2) systematic differences between the LRIS and

Smoothed HIRES spectra. Any residual differences in the wavelength scales in the two spectra will produce greater than random scatter in the resulting spectrum. The scatter does increase towards lower wavelengths, and this is most likely due to decreasing SNR with decreasing wavelengths, and intrinsic features in the QSO spectrum. Our guess at the systematic error in the continuum is shown as the dotted lines in Figure 3. Assuming the unabsorbed continuum can be modeled as a low order polynomial, the slope of the continuum in the region of interest is much better determined than the absolute level. Even with these conservative estimates, the continuum is known to better than 10% over the full spectral range in Figure 3. We extrapolate the fit from 4200 Å to 3850 Å, which is the region where the flux level drops due to the Lyman limit at  $z = 3.572$ .

With large optical depths,  $N(\text{H I})$  is fairly insensitive to the placement of the continuum. A small error in the continuum,  $\Delta I_0$ , would result in a proportional error in the column density of

$$\frac{\Delta N(\text{H I})}{N(\text{H I})} = \frac{\Delta I_0}{\tau}, \quad (1)$$

which is reduced by the optical depth of the absorption. In our case, a 10% error in the continuum level ( $\Delta I_0 = 0.1$ ) for an optical depth of  $\tau_c = 4.6$ , contributes an additional 2% uncertainty in  $N(\text{H I})$ . This error is approximately one-half the magnitude of the statistical error discussed in the next section.

#### 4. $N(\text{H I})$ Column Density

The total neutral hydrogen column density,  $N(\text{H I})$ , can be measured from the Lyman continuum optical depth,  $\tau(\lambda) = -\text{Ln}(I_\lambda/I_0)$ , where  $I_0$  is the unabsorbed flux, and  $I_\lambda$  is the absorbed flux blueward of the Lyman limit at  $\lambda_0 = 911.75(1 + z_{abs})$  Å. The hydrogen photoionization cross-section has an energy dependence which gives an optical depth as a function of wavelength of

$$\tau(\lambda) \approx \frac{N(\text{H I})}{1.6 \times 10^{17} \text{cm}^{-2}} \left( \frac{\lambda}{\lambda_0} \right)^{2.7} \quad (2)$$

(Osterbrock 1989).

If the absorption system at  $z = 3.572$  was the only one with significant absorption at  $\lambda < 4200$  Å, we could fit eqn. 2 to the LRIS spectrum. However we must first account for extra absorption, which can be placed into two groups, (1) the absorption of higher-order Lyman lines ( $\text{Ly}\beta$ ,  $\text{Ly}\gamma$ ,  $\text{Ly}\delta$ , ...) and Lyman continuum from high redshift systems ( $2.75 < z < 3.572$ ), and (2) Lyman- $\alpha$  absorption falling directly in the region of interest ( $2.16 < z < 2.45$ ). Absorption by hydrogen systems at higher redshifts ( $3.572 < z < 3.78$ )

has already been accounted for in the calculation of the quasar continuum, because all their Lyman series lines and Lyman continuum absorption lie at wavelengths greater than 4200 Å, where the HIRES spectrum has high SNR. The group (1) absorption can be directly identified from the Ly $\alpha$  lines in regions of the HIRES spectrum where the SNR is high. We fit Voigt profiles to measure the absorption parameters for all systems in group (1) (Burles 1997). The corresponding Ly $\beta$ , Ly $\gamma$ , Ly $\delta$ , ..., and Lyman continuum absorption is shown in Figure 4.

Absorption from group (2) cannot be directly measured, because the SNR is below one in the HIRES spectrum blueward of the Lyman limit. We used Monte Carlo methods to statistically account for this absorption, and to determine simultaneously the likelihood of the data as a function of the N(H I) at  $z = 3.572$ . We step through a range of N(H I) values, and generate 10000 model spectra for each value of N(H I). All models had the same absorption from the systems in group 1, but each had a different realization of the group (2) Ly $\alpha$  lines, drawn from the known distribution of Ly $\alpha$  lines (Kirkman & Tytler 1997). Each model spectrum was compared to the data, and the probability of each model was calculated with the  $1\sigma$  error array. The resulting likelihood function is shown in Figure 5. The most likely value for the total N(H I) is  $\text{Log} [\text{N(H I)}] = 17.86 \text{ cm}^{-2}$ . Near the maximum likelihood, the function is nearly Gaussian and gives a  $1\sigma$  error of 0.015 in logarithmic units. Figure 4 shows the residual flux below 4200 Å, and the model fit with  $\text{N(H I)} = 17.86 \text{ cm}^{-2}$  plus the additional absorption from group 1, but not the absorption from group 2. Adding the uncertainty from the continuum level to the likelihood function in Figure 5, we find  $\text{Log} [\text{N(H I)}] = 17.86 \pm 0.02 \text{ cm}^{-2}$ .

## 5. Comparison of N(H I) Measurements

TFB measured the line profiles of all uncontaminated Lyman lines and found  $\text{Log} [\text{N(H I)}] = 17.94 \pm 0.05 \pm 0.06 \text{ cm}^{-2}$ , where the first error is statistical and the second is systematic. Now using different instruments and methods, we find an independent measure of  $\text{Log} [\text{N(H I)}] = 17.86 \pm 0.02$ , which agrees.

Songalia et al. (1997) used a similar LRIS spectrum, and reported a “reasonable maximum”,  $\text{Log} [\text{N(H I)}] < 17.7 \text{ cm}^{-2}$ . The inconsistency between the two results arises from the different methods of analysis. We present four reasons for this inconsistency. (1) Lacking high-resolution spectra, they relied on statistical models to determine the unabsorbed quasar continuum. They proposed two models, both of which underestimate the unabsorbed continuum which we have measured. In their Figure 2, their model continua pass below their data, which is unphysical. (2) They do not include most of the absorption

systems in groups 1 or 2. (3) Instead of using all the  $\approx 350$  pixels in the Lyman limit region, they measure  $\tau$  from a region with less than 20 pixels. (4) They did not include the energy dependence in the hydrogen photoionization cross-section, which gives a 7% underestimate of  $N(\text{H I})$ .

Our LRIS spectrum is apparently consistent with theirs. A direct comparison of the data is difficult, because they do not present their data with absolute flux units. We transformed our fluxed LRIS spectrum into Log Flux in units of energy per unit frequency. We see the same features, the same slope in flux, and the same decrease below the Lyman limit. In Figure 6, we show our LRIS spectrum with the same relative scale and the same spectral resolution as their Figure 2a spectrum. We measure the average flux blueward of  $4200 \text{ \AA}$  at  $\text{Log Flux} = 0.7$ , which appears to be consistent with their LRIS spectrum.

Our result is not consistent with the alternative models proposed by Wampler (1996). His models require large systematic errors in the sky subtraction of the HIRES spectrum presented by TFB. The models do not agree with the data for the following reasons: The spectrum was optimally extracted using automated routines written by Tom Barlow. All optically thick Lyman Lines are black at their line centers in the HIRES spectrum, which is a good check on the sky subtraction. In addition, two LRIS spectra (Songaila’s and ours) both show the same flux below the Lyman limit, and giving an  $N(\text{H I})$  which is 50% too large for Wampler’s models.

We directly determined the intrinsic unabsorbed quasar continuum using three independent spectra, and measured the optical depth of the Lyman limit at  $z = 3.572$ . We find  $\text{Log } [N(\text{H I})] = 17.86 \pm 0.02$ , where the error includes both photon noise and uncertainty in the continuum. The result is consistent with that which we determined from fitting the Lyman series lines in the HIRES spectrum (TFB). With this new constraint, we can now provide a better measurement of  $D/H$  in this absorption system. The  $N(\text{D I})$  reported by TFB cannot be used because the deuterium and hydrogen profiles are blended (i.e. changing  $N(\text{H I})$  will change  $N(\text{D I})$ ). Our improved analysis of the high-resolution spectra with this new constraint will be presented in Burles & Tytler (1997).

We are very grateful to Charles Steidel for obtaining the LRIS observations. We thank Tom Barlow, David Kirkman, and Jason X. Prochaska for many helpful suggestions.



## REFERENCES

- Adams, T. F., 1976, A&A, 50, 461
- Burles, S. 1997 in preparation
- Burles, S., Kirkman, D. & Tytler, D. 1997 in preparation
- Burles, S., & Tytler, D. 1996, astro-ph 9603070
- Burles, S., & Tytler, D. 1997, submitted to AJ
- Burstein, D. & Heiles, C. 1984, ApJS, 54, 33
- Copi, C. J., Schramm, D. N., & Turner, M. S. 1995, Science, 267, 192.
- Kirkman, D., & Tytler, D. 1997, ApJ, in press.
- Lu, L., & Zuo, L. 1994, ApJL, 426, 502
- Osterbrock, D. E. 1989, Astrophysics of Gaseous Nebulae and Active Galactic Nuclei (Mill Valley, CA: Univ. Sci.)
- Songaila, A., Wampler, E. J., & Cowie, L. L. 1997, Nature, 385, 137
- Tytler, D., & Burles, S. 1996, in *Origin of Matter and Evolution of Galaxies* eds. T. Kajino, Y. Yoshii & S. Kubono (World Scientific Publ. Co., 1996) (astro-ph 9606110)
- Tytler, D., Fan, X-M., & Burles, S. 1996, 381, 207 (TFB)
- Wampler, E. J. 1996, Nature, 383, 308
- Zheng, W., Kriss, G., Telfer, R. C., Grimes, J. P., & Davidsen, A. F. 1997, ApJ, 475, 469

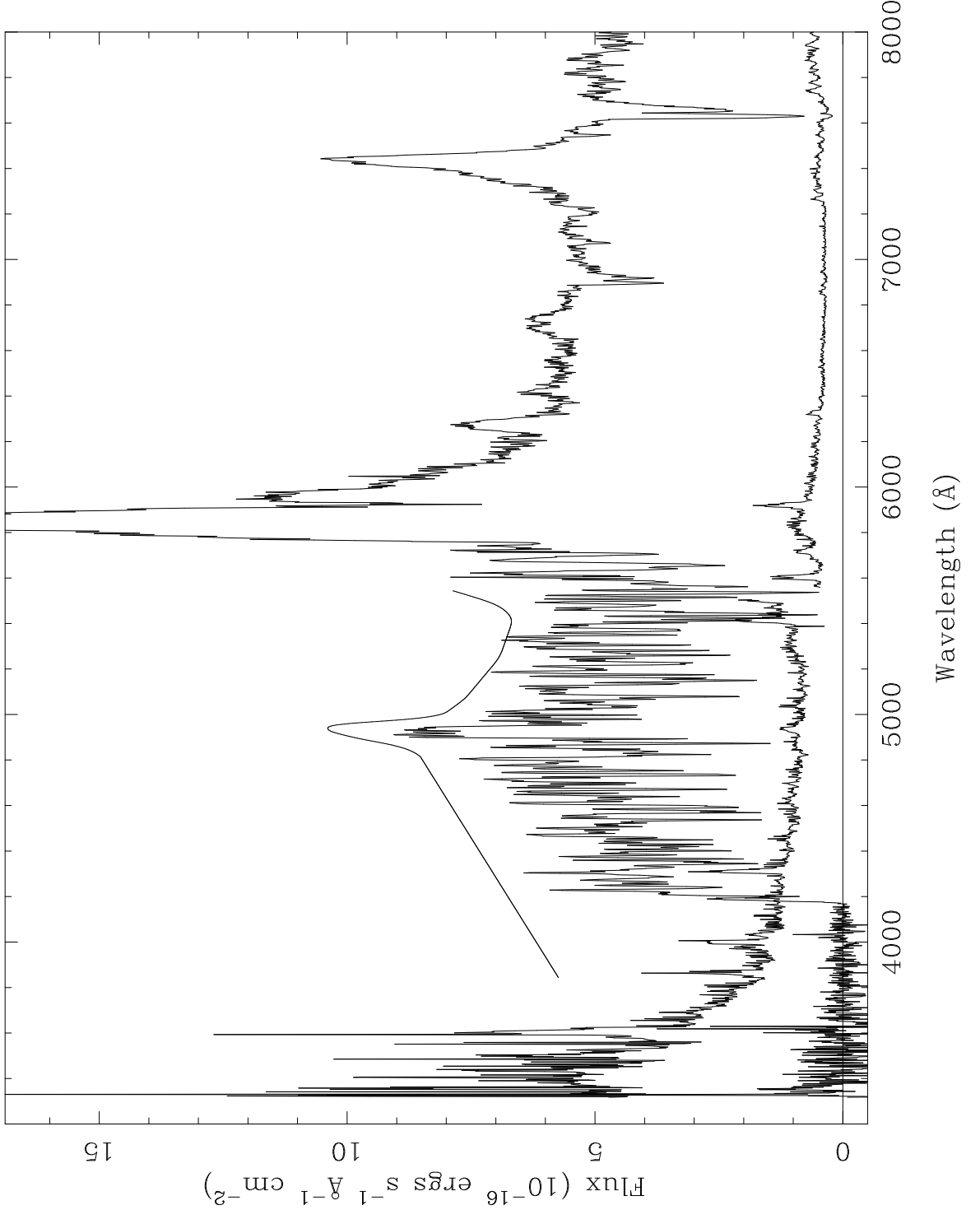


Fig. 1.— A wide slit spectrum of Q1937-1009 ( $z_{em} = 3.805$ ,  $V = 17.5$ ) obtained at the Lick Observatory Shane 3-m telescope with the Kast spectrograph. This spectrum was used to flux calibrate the LRIS spectrum. We show the unabsorbed quasar continuum (the smooth solid line) for reference. The  $10\sigma$  error is also plotted, which is  $\simeq 1.5$  at 4000  $\text{Å}$ .

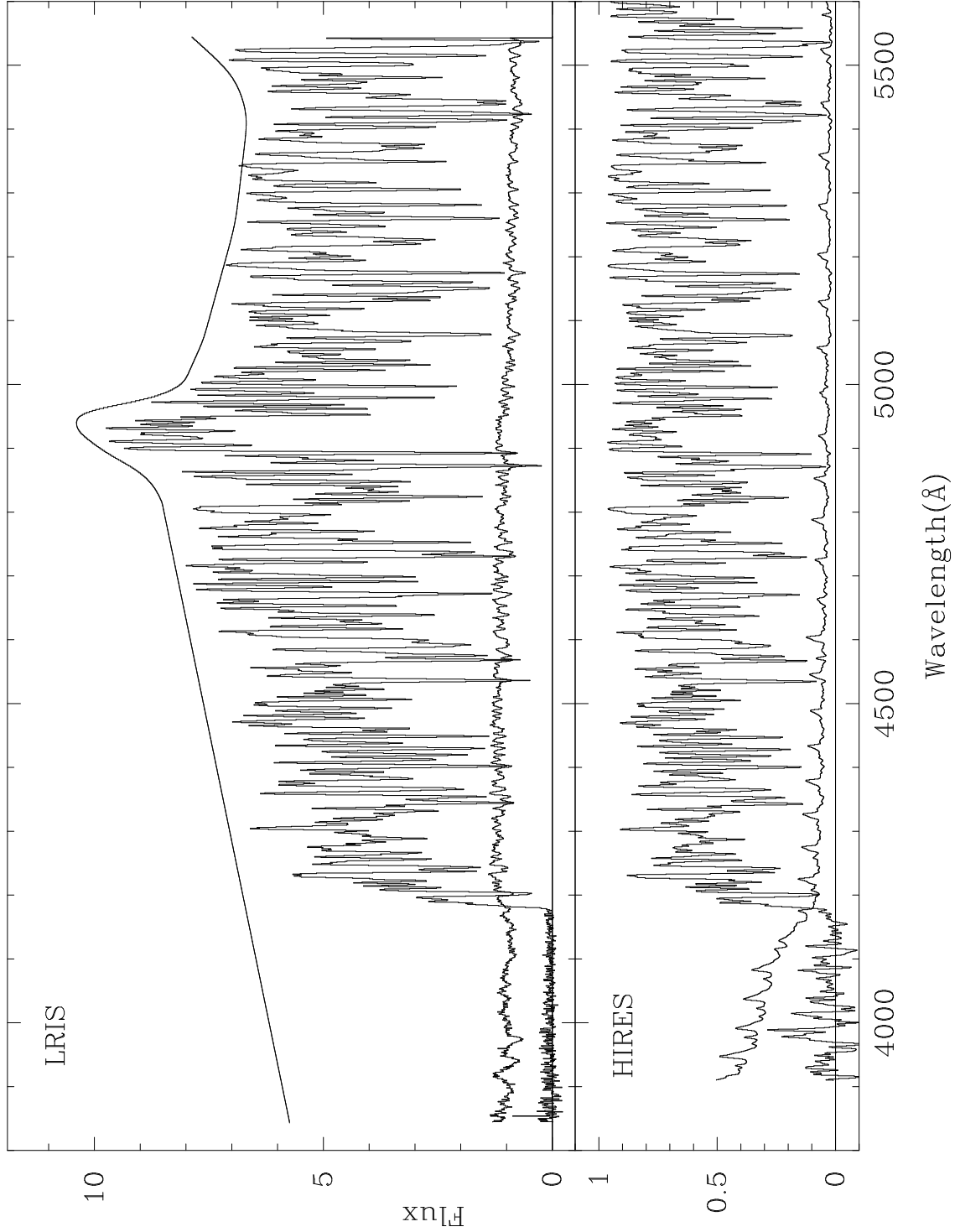


Fig. 2.— The top panel shows the spectrum of Q1937–1009 obtained at the 10-m W.M. Keck 1 Telescope with the Low Resolution Imaging Spectrograph (LRIS). The flux is in units of  $10^{-16} \text{ ergs s}^{-1} \text{ cm}^{-2} \text{ Å}^{-1}$ . We also show the accompanying  $10\sigma$  error, which is  $\simeq 1.0$  at 4000 Å. The bottom panel shows the HIRES data rebinned to LRIS pixels and smoothed to the LRIS resolution (3 Å FWHM). The HIRES spectrum has been normalized with the unabsorbed quasar continuum set to 1. We show the weighted  $10\sigma$  error per LRIS pixel, which is  $\simeq 0.35$  at 4000 Å.

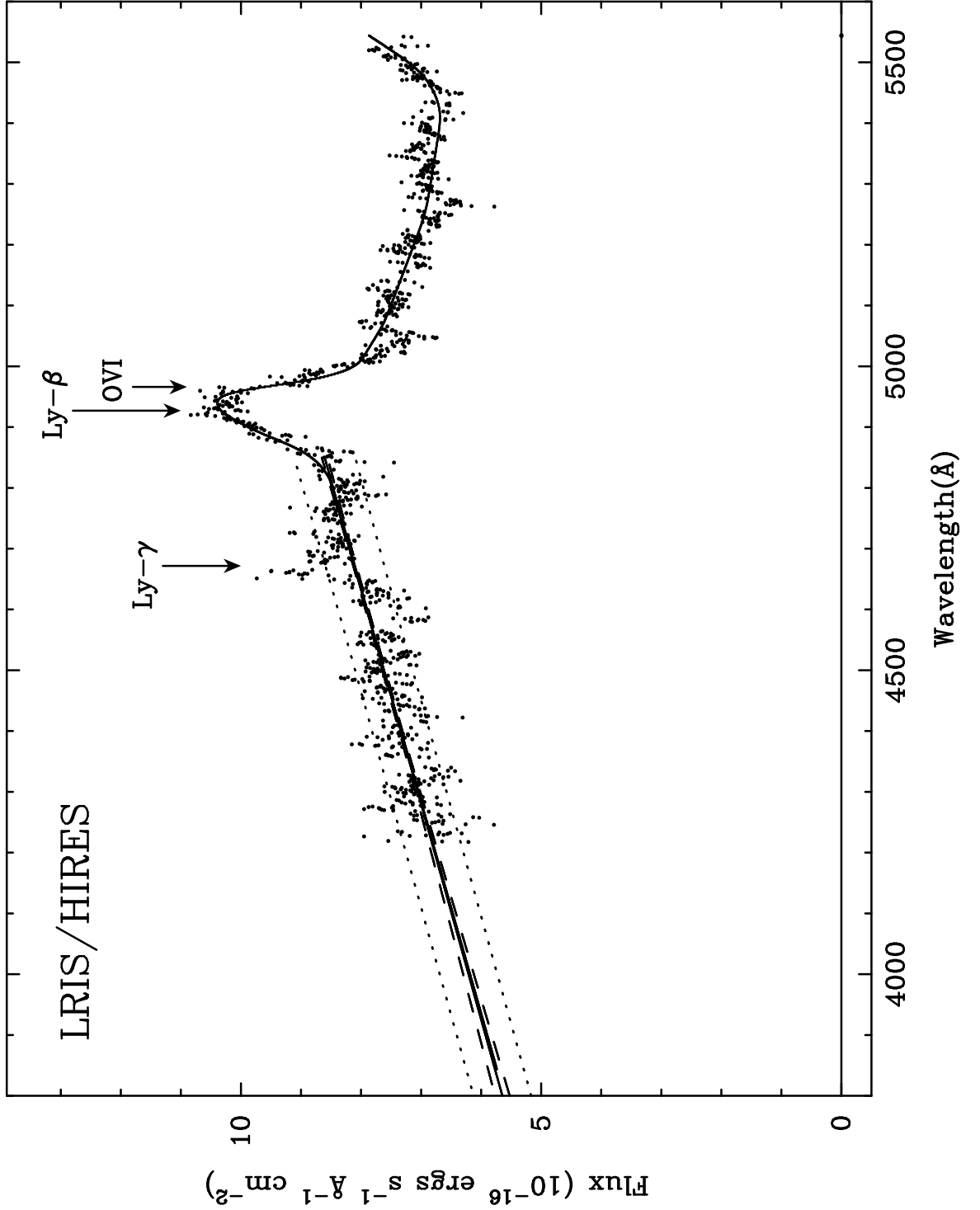


Fig. 3.— The LRIS spectrum divided by the HIRES spectrum. The points are pixels, and the smooth solid line is the adopted unabsorbed continuum. The dashed lines show the  $1\sigma$  uncertainties in the linear fit to the continuum below 4850 Å. Dotted lines indicate guessed systematic errors.

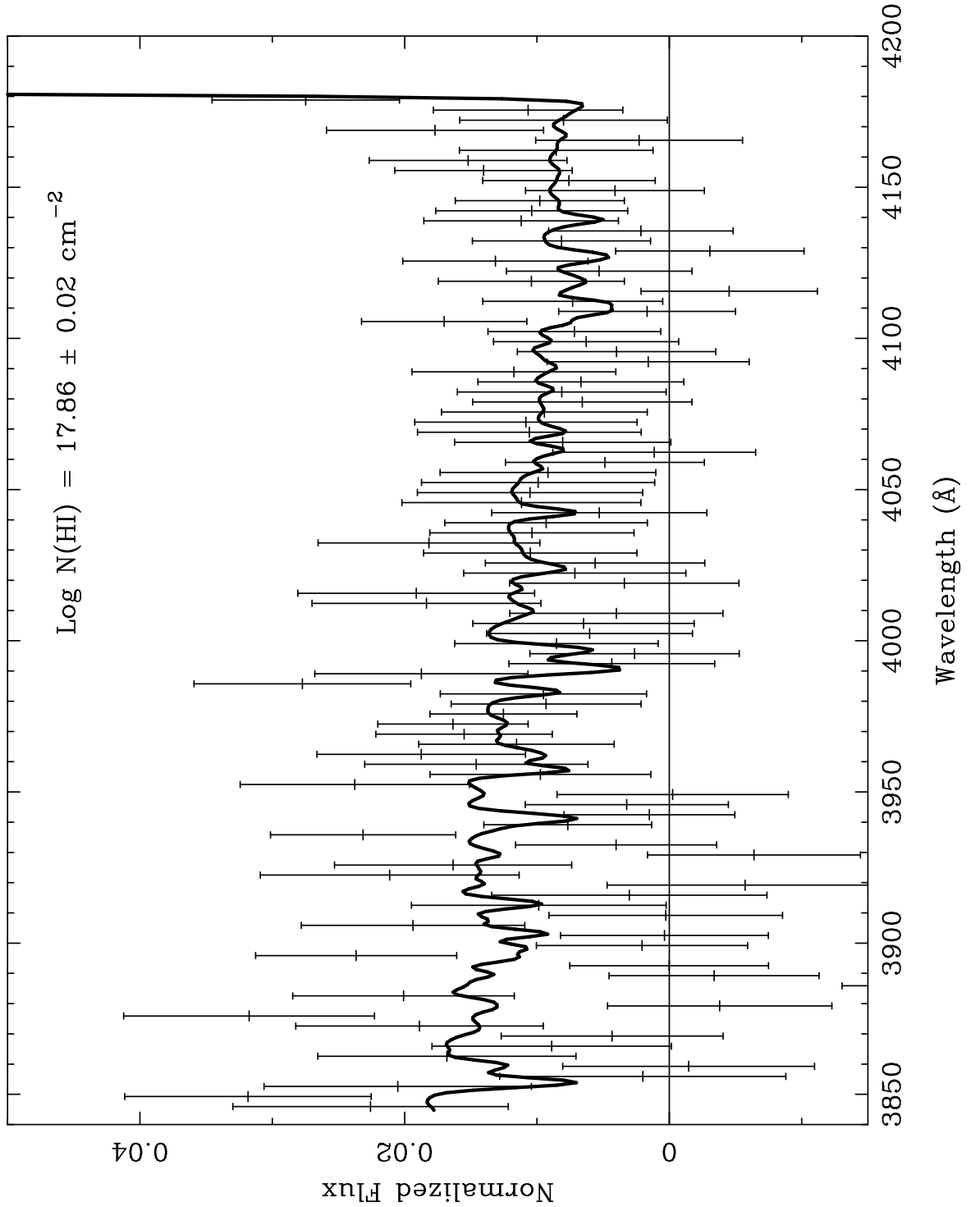


Fig. 4.— The portion of the LRIS spectrum showing residual flux below the Lyman limit at  $z = 3.572$ . The data is shown as normalized flux with  $1\sigma$  error bars, and is binned over 4 pixels for display purposes only. The fit of maximum likelihood is the solid curve corresponding to  $\text{Log } [N(\text{H I})] = 17.86 \text{ cm}^{-2}$ .

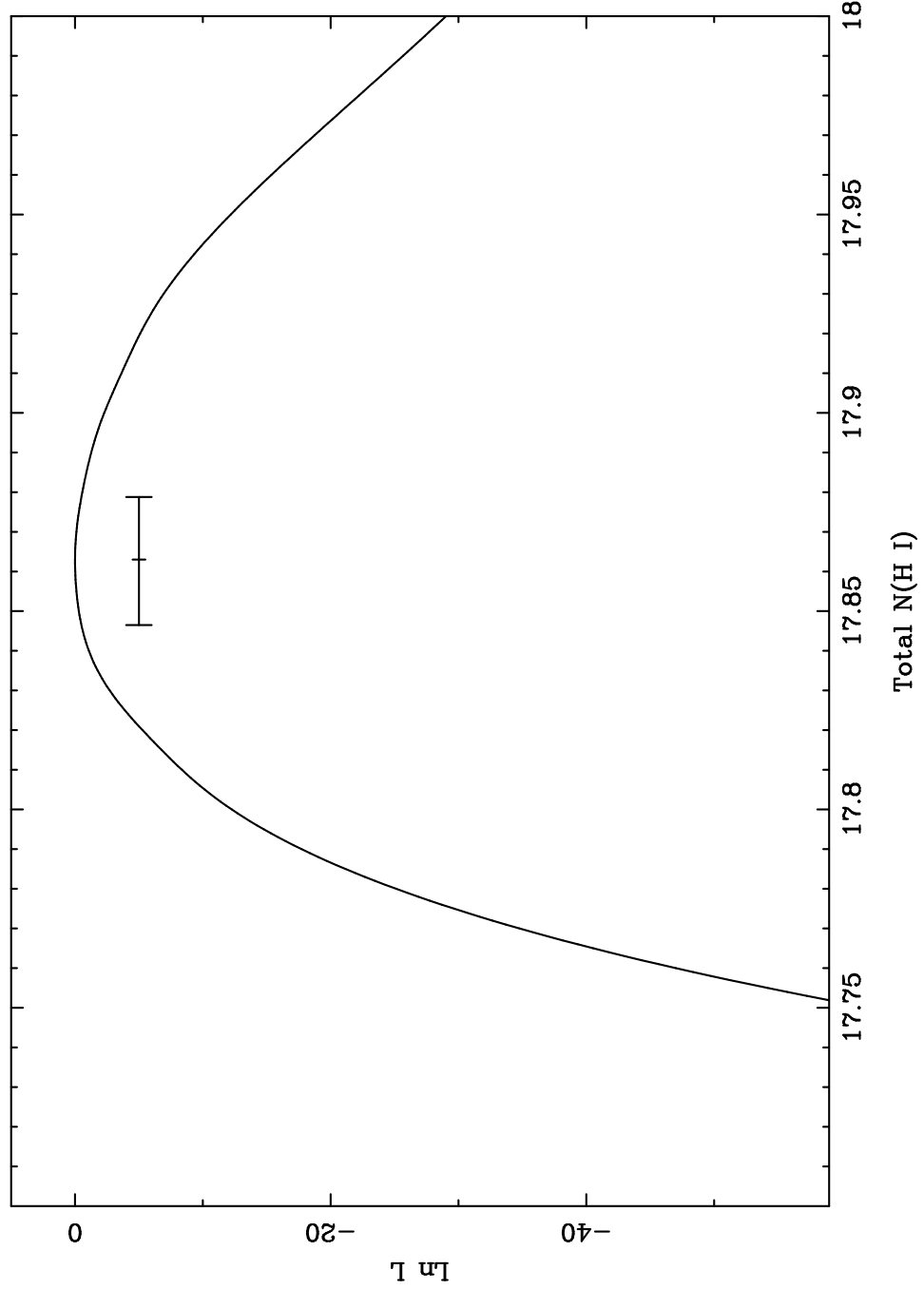


Fig. 5.— Likelihood function of  $N(\text{H I})$  from simulations of the LRIS data. The maximum likelihood is at  $\text{Log } [N(\text{H I})] = 17.863 \text{ cm}^{-2}$ , with a 67% confidence levels at  $\text{Log } [N(\text{H I})] = 17.848 \text{ cm}^{-2}$  and  $17.878 \text{ cm}^{-2}$ .

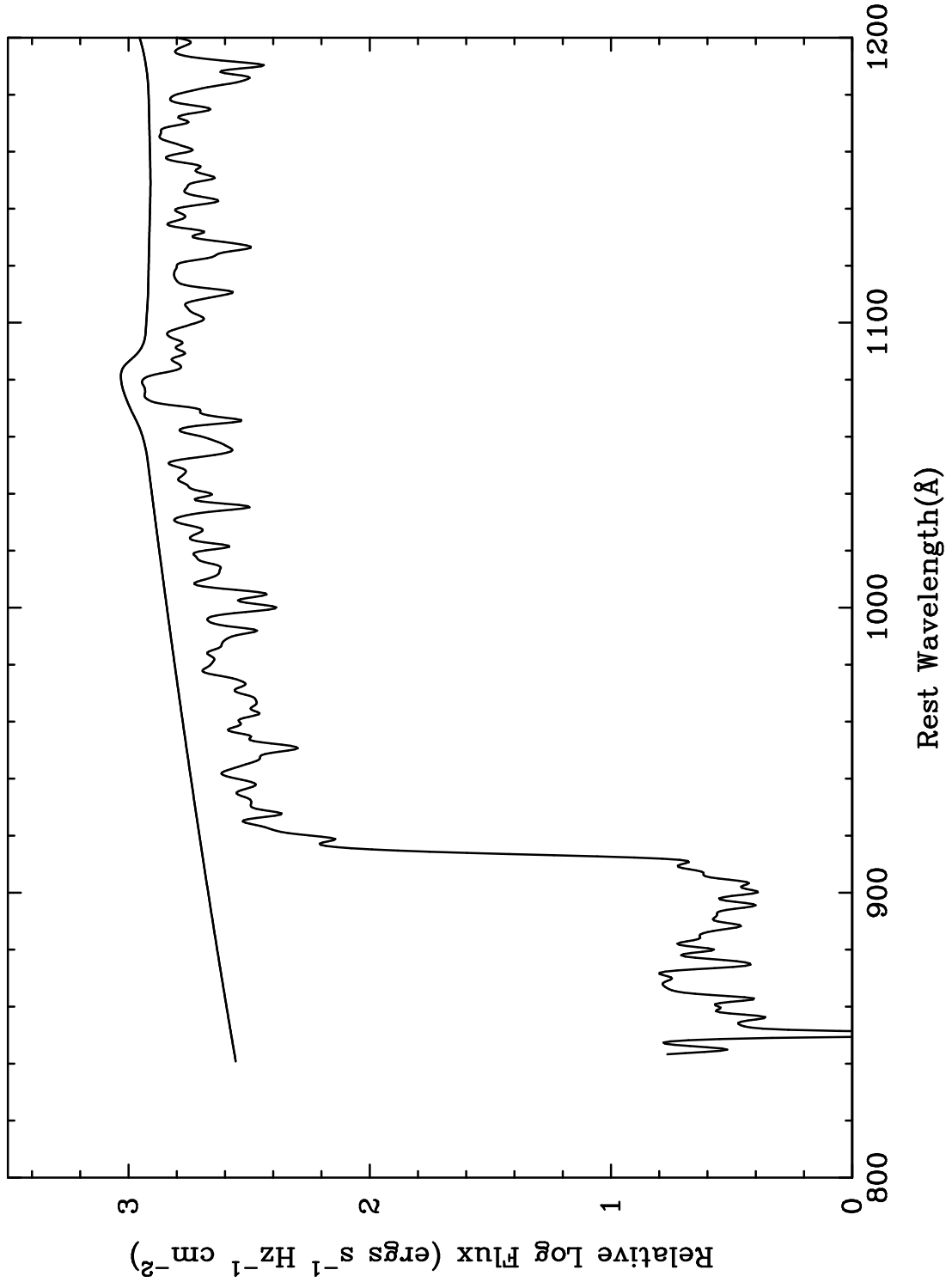


Fig. 6.— The LRIS spectrum shown in Figure 2 plotted in Relative Log Flux in energy per unit frequency versus rest wavelength at  $z = 3.572$ . The smooth line is the intrinsic unabsorbed quasar continuum shown in Figure 3. This figure is intended to facilitate a comparison of our LRIS data with that presented by Songaila et al. (1997) in their Figure 2a.